Magnetism in orbitally unquenched chainar compounds. II. The ferromagnetic case: $RbFeCl_3$

M. Eibschütz, M. E. Lines, and R. C. Sherwood
Bell Laboratories, Murray Hill, New Jersey 07974
(Received 16 December 1974)

Measurements of quadrupole splitting by the Mössbauer effect and of single-crystal magnetic susceptibility are reported for the ferromagnetic chainar crystal $RbFeCl_3$. By use of crystal-field theory and the correlated-effective-field statistical approximation these results are analyzed in terms of a model with only three adjustable parameters, a spin-orbit coupling constant, a trigonal crystal-field parameter, and an intrachain Heisenberg exchange J between real spins. A quantitative analysis paralleling that used in a previous paper for isomorphic $RbFeBr_3$ is less successful in the present case, discrepancies arising at low temperatures which are at least partly due to small interchain exchange. The latter, which for $RbFeCl_3$ perturbs a quasi*ferro* magnetic system in an *antiferro* magnetic fashion, produces qualitative effects on magnetic response at sufficiently low temperatures. In addition, we suggest possible evidence for the importance of a non-Heisenberg contribution to exchange, the form and origin of which are discussed.

I. INTRODUCTION

In Paper I of this series we discussed $RbFeBr_3$ and were able to obtain a fairly quantitative understanding of linear-chain antiferromagnetism in this orbitally unquenched Fe^{2+} system by use of the correlated-effective-field (CEF) theory. In this paper we consider isomorphic $RbFeCl_3$, concerning which there is already a conflicting literature, as described in Paper I. The prime reason for reporting the bromide study first is that it appears *a posteriori* to be the simpler problem; in fact the quality of the over-all self-consistency and agreement with experiment for the bromide seems if anything to be better than one might reasonably anticipate for a chainar system of this complexity. The equivalent approach for the chloride meets with more modest success and, although we shall be able to improve quite considerably upon the earlier efforts to understand the magnetic aspects of the material, our analysis suggests that orbitally degenerate exchange and small interchain interactions play much enhanced roles in $RbFeCl_3$ at low temperatures and make a quantitative theoretical analysis that much more difficult to obtain.

The absolute magnitude of the (antiferromagnetic) interchain forces in $RbFeCl_3$ is still very small compared to intrachain exchange but they now perturb a quasiferromagnetic chainar system (as opposed to a quasiantiferromagnetic chainar system in $RbFeBr_3$) and are able to produce qualitative effects at low temperatures which seemingly cannot adequately be described by introducing them as small perturbational effective fields. Non-Heisenberg exchange is probably absolutely larger in the chloride by virtue of the shorter c-axis direct iron-iron distance (orbitally degenerate exchange occurring from direct c-axis overlap as detailed later in the text), but perhaps of equal importance is the fact that the Heisenberg and non-Heisenberg contributions to exchange are of opposite sign in $RbFeCl_3$ leading to cancellation effects.

In Sec. II we describe the experimental measurements of quadrupole splitting and single-crystal magnetic susceptibility taken on $RbFeCl_3$. Section III analyzes these results using a theory which assumes an intrachain exchange of dominantly Heisenberg form between real spins. The analysis is adequate at higher temperatures but appears to fail below about 60 °K for a variety of reasons. Allowance for the expected inaccuracy of the statistical (CEF) approximation at lower temperatures and for the inclusion of interchain exchange improves the situation but discrepancies remain which appear to require the introduction of orbitally degenerate exchange. An approximate representation for the latter is derived from physical principles in Sec. IV and the resulting statistical problem solved within the CEF approximation in Sec. V. Section VI reanalyzes the experimental data using the orbitally degenerate theory and concludes that there is fairly persuasive evidence in favor of the breakdown of the Heisenberg formalism in $RbFeCl_3$.

II. EXPERIMENTAL

The preparation of the $RbFeCl_3$ material and the growing of single crystals have already been described by Cox and Merkert.[1] In summary, the material was prepared by careful dehydration and reduction of a solution of Rb_2CO_3 and Fe_2O_3 in dilute HCl. Single crystals up to 1 cm^3 in volume were grown by the Bridgman technique. The crystals had (100) cleavage planes.

The experimental techniques used for obtaining

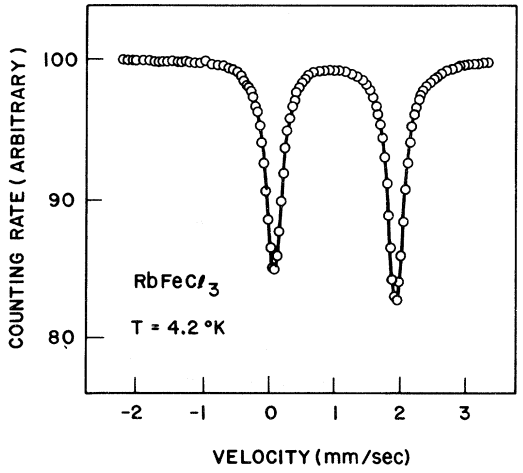

FIG. 1. Characteristic Mössbauer quadrupole spectrum for $RbFeCl_3$. The source was ^{57}Co in Pd.

the Mössbauer-effect (ME) absorption spectra have already been described in Paper I. The ^{57}Fe ME absorption spectra in powder samples at 4.2 °K and above show two resonance lines due to the electric field gradient at the iron nucleus. A characteristic ME spectrum is shown in Fig. 1. The slight asymmetry in the line intensities of the spectrum may be due to a possible nonrandom orientation of small single-crystal platelets in the powder sample. The spectra were analyzed by fitting to a sum of two Lorentzian curves of independent position, width, and dip. The quadrupole splitting results are shown in Figs. 3 and 12.

The sign of the quadrupole splitting (QS) was inferred from the asymmetry of the peak intensities observed using an absorber made of up of a mosaic of (100) single-crystal platelets. With an axially symmetric geometry the ratio of the area of the low-velocity line to that of the high-velocity line should be 3:5 for $\frac{1}{2}e^2qQ<0$ or 5:3 for $\frac{1}{2}e^2qQ>0$ in conventional notation.[2] We observed a ratio of 0.64 at 4.2 °K and hence conclude that the QS is negative. This sign is consistent with that required to fit the ME spectra below the three-dimensional ordering of the material.[3] Since the Fe^{2+} ion is at a site of D_{3d} symmetry the negative sign implies that the ground-state wave function is of orbital singlet character, in agreement with our analysis of the susceptibility data.

Spectra below the three-dimensional ordering of the material ($T_N = 2.55 \pm 0.05$ °K) are magnetically split into an apparent doublet and an apparent triplet, a result characteristic of a small hyperfine field directed perpendicular to the electric-field-gradient principal axis. The spectra in the magnetic state have already been studied and published.[3]

Magnetic-susceptibility single-crystal measurements between 1.5 and 300°K were taken using a pendulum magnetometer. The resulting curves for $RbFeCl_3$ in a field of 15.3 kOe are shown in Fig. 2, where we also plot reciprocal parallel and perpendicular susceptibilities to demonstrate their linearity above $T \sim 100$ °K.

III. ANALYSIS

Since $RbFeCl_3$ is isomorphic with $RbFeBr_3$ the formal crystal-field analysis of Paper I is directly applicable for the chloride as well. If also, initially, we assume a simple Heisenberg exchange between real spins $\vec{S}$, we arrive at Eq. (4.5) of Paper I for the spin Hamiltonian operator for an Fe^{2+} ion at site i, viz.,

$$\mathcal{H}_i = \Delta'(L_{iz}'^2 - \tfrac{2}{3}) + |\lambda| \vec{L}_i' \cdot \vec{S}_i - \sum_j 2J \vec{S}_i \cdot \vec{S}_j . \quad (3.1)$$

In this equation (see Paper I) $L' = 1$, $S = 2$ label the 15 states of the lowest T_2 orbital triplet of Fe^{2+} in octahedral symmetry, Δ' is a crystal-field trigonal

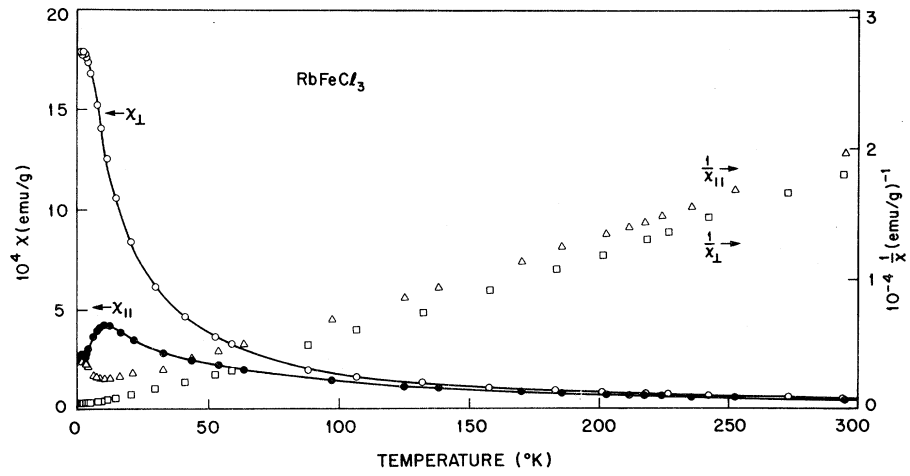

FIG. 2. Single-crystal magnetic susceptibility curves for $RbFeCl_3$. Also shown are plots of reciprocal susceptibility to demonstrate their linearity and parallel character at higher temperatures.

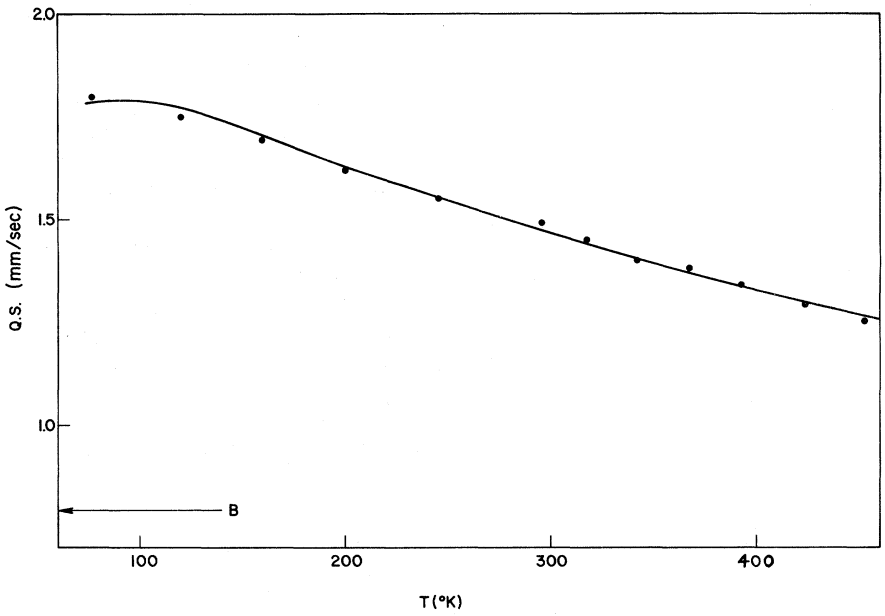

FIG. 3. Higher temperature quadrupole splitting for $RbFeCl_3$ (filled circles) is fitted to the theoretical form $A\langle L_z^2 - 2\rangle + B$ with spin-orbit coupling $|\lambda| = 130\,°K$ and trigonal distortion $\Delta'/|\lambda| < 3$ (see text).

distortion, λ is a spin-orbit coupling parameter, and J is an intrachain isotropic Heisenberg exchange between real spins. From the measured single-crystal magnetic susceptibility we find the c axis (or z axis) to be a hard direction and expect correspondingly that Δ' will be positive, giving a singlet-ground-state configuration (Fig. 5 of Paper I).

Using (3.1) we neglect at this point any interchain exchange and any orbitally degenerate contribution to exchange. Such assumptions are consistent with those used successfully in Paper I for the bromide. The previous efforts in the literature to interpret the low-temperature susceptibility of $RbFeCl_3$ have also started with these assumptions but, in addition, have derived a fictitious spin-1 Hamiltonian to concentrate only on the lowest three iron levels, the ground singlet and an excited doublet of order 10 cm^{-1} above. At sufficiently low temperatures there is nothing in principle wrong with this but great care must be taken; for example, the Van Vleck temperature-independent contribution to susceptibility arising from the matrix elements connecting the lowest three states to the next highest levels some 200–300 cm^{-1} away are far from negligible, and the effective g values are not independent parameters but are essentially determined by the value of trigonal distortion via crystal-field theory. The analysis of Montano *et al.*[4] in particular suffers in both these respects, neglecting a Van Vleck term which we shall show to be fully 25% of the c-axis susceptibility at 70 °K and obscuring the statistical breakdown of the pair model at low temperatures by adjusting g values in a manner which even qualitatively violates crystal-field theory. For example Montano's best-fit g values $g_{\parallel} = 3.52$, $g_{\perp} = 2.90$ are in conflict with the crystal-field requirement that $g_{\parallel} < g_{\perp}$ in the spin-1 formalism when $\Delta'/|\lambda|$ is positive.

In this paper we shall again use the CEF statistical theory of magnetism,[5] which has already been successfully used on $RbFeBr_3$ and which has been quantitatively compared in Paper I with the best existing chainar theories in the simple spin-only magnetic context for which more accurate schemes are available. In this theory it is not necessary to develop the fictitious spin-1 representation and as a result the higher-temperature measurements can be included in the analysis. The CEF approximation in the present context has been set out in detail in Paper I and need not be repeated. As with the bromide we analyze first the nuclear quadrupole splitting at temperatures above ~100 °K, for which CEF theory indicates that exchange of the order of magnitude expected for the hexagonal ABX_3 compounds plays no measurable role. The experimental splitting between 100 and 450 °K is fitted to an expression $A\langle L_z^2 - 2\rangle + B$ as explained in Paper I. where $\vec{L}$ is the real angular momentum operator ($L_z^2 = 3L_z'^2$ in the lowest T_2 triplet) and the constant term B is usually attributed to a lattice (crystal-field) contribution. Theoretically, for values of $\Delta'/|\lambda|$ between 0 and about 3, the higher-temperature $\langle L_z^2 - 2\rangle$ curves scale very closely with amplitude and a good fit to the scaled curve (see Fig. 3) can be obtained if B is of the same sign as $A\langle L_z^2 - 2\rangle$ and of magnitude 0.79 ± 0.09 mm/sec, and if spin-orbit coupling constant $|\lambda| = 130 \pm 10$ °K (90 ± 7 cm^{-1}). This fixes the orbital-reduction

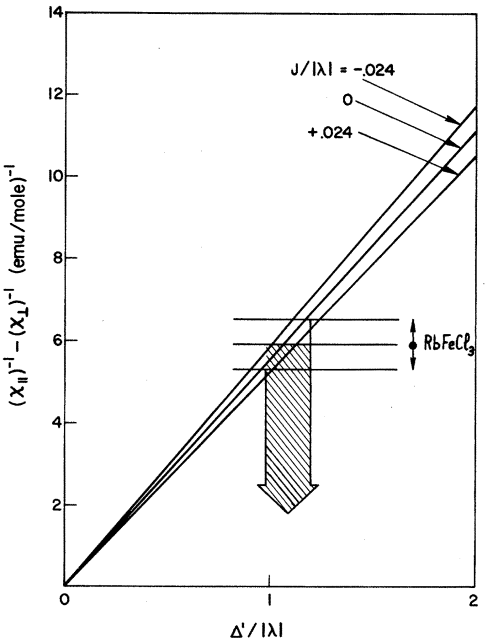

FIG. 4. CEF curves of the difference between reciprocal-parallel susceptibility and reciprocal perpendicular susceptibility are shown as a function of $\Delta'/|\lambda|$ for temperature $kT/|\lambda| = 2$, and an orbital reduction parameter $k = 0.87$. The constant experimental high-temperature value of this difference, as taken from Fig. 2, is shown by the filled circle and error bars. The arrow centered on $\Delta'/|\lambda| = 1.1$ records the value of trigonal splitting consistent with experiment for small ferromagnetic exchange $J/|\lambda| \sim +0.01$.

parameter k, which is the ratio of $|\lambda|$ to its free-ion value of 103 cm^{-1}, as $k = 0.87 \pm 0.07$.

The value of k for $RbFeCl_3$ is therefore a little larger than for $RbFeBr_3$ and conforms with the qualitative expectation that the chloride should be less covalent. The values of B in the two materials are not significantly different but do not seem to conform with crystal-field estimates (crude though the latter may be) for a lattice contribution either in magnitude or sign. We shall not pursue the possible microscopic origin of B except to note that a very significant temperature-independent term could arise from the orbital electrons themselves if allowance were made for possible inequivalence of radial distribution in the $L_g' = 0$ and $L_g' = \pm 1$ orbitals by virtue of their very different local environments.

Using an orbital-reduction parameter $k = 0.87$ and writing magnetic moment $\vec{\mu} = 2\vec{S} + k\vec{L} = 2\vec{S} - k\vec{L}'$ we can now compute the CEF susceptibility curves as functions of trigonal distortion and exchange alone. At temperatures above about 100 °K the experimental difference between reciprocal parallel and reciprocal perpendicular susceptibilities is approximately independent of temperature and equal to 5.9 ± 0.6 (emu/mole)$^{-1}$. At these higher temperatures the effects of exchange are minor and a fit of theory with experiment determines the single parameter $\Delta'/|\lambda|$ quite precisely. In Fig. 4 we show the high-temperature splitting $\chi_{\parallel}^{-1} - \chi_{\perp}^{-1}$ as computed by CEF theory. A fit to the experimental observation gives $\Delta'/|\lambda| = 1.1 \pm 0.1$. At lower temperatures the susceptibility becomes sensitive even to small values of exchange J and we show the computed CEF low-temperature curves for parallel and perpendicular susceptibility in Fig. 5. In this same figure we plot the experimental measurements both as taken by ourselves and as published by Achiwa.[6] Although minor differences are apparent between the two sets of measured values it is evident that neither set can be fitted by any J-value exchange if $\Delta'/|\lambda| = 1.1 \pm 0.1$. Nor is the over-all situation significantly improved by allowing $\Delta'/|\lambda|$ to take values outside this range, although the $\chi_{\parallel}$ picture can be improved by taking a slightly larger value $\Delta'/|\lambda| \sim 1.5$.

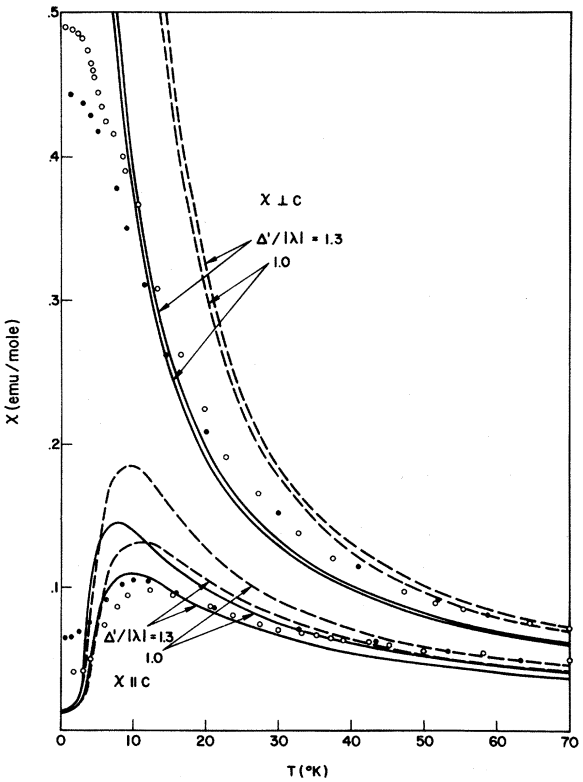

FIG. 5. CEF curves of parallel and perpendicular susceptibility as a function of temperature are compared with the experimental measurements of Achiwa (open circles) and of ourselves (closed circles) for single-crystal $RbFeCl_3$. The theoretical curves are calculated with $|\lambda| = 130$ °K, $k = 0.87$, and for values of exchange $J/|\lambda| = 0$ (full curves) and $J/|\lambda| = 0.01$ (dashed curves).

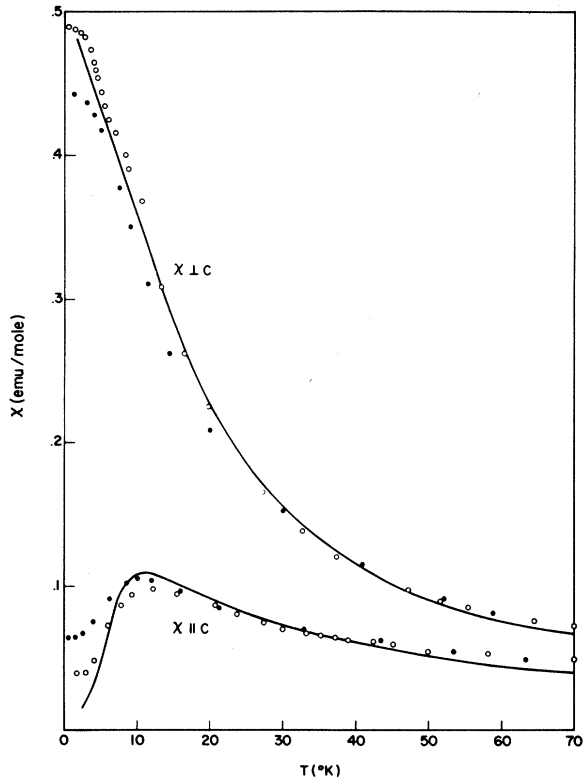

FIG. 6. Best fit of CEF theory with the experimental points of Fig. 5, obtained by including in the calculation an effective field representing *inter*chain interreactions. See text for details.

One undeniable shortcoming of the theory is the too rapid increase of $\chi_\perp$ as the temperature is decreased. This property is present even in pair-model theory, which should underestimate low-temperature response (Fig. 4 of Paper I). Montano *et al.*[4] attempt to adjust for this by lowering the perpendicular g factor (a degree of freedom denied us by crystal-field self-consistency) but this only transfers the discrepancy to high temperatures (Fig. 5 of Ref. 4). One obvious possible solution is to allow for interchain interactions. These are of antiferromagnetic sign (as may be discerned from the spin arrangement in the ordered phase below $T \approx 2.5\,^\circ$K) and therefore slow the diverging character of $\chi_\perp$ as T is lowered and eventually arrest the rise completely when long-range order sets in. To include interchain exchange self-consistently within the CEF approximation would increase the computational complexity very significantly but it can be included as an effective field relatively simply.

Let the magnetic moment per site, under the influence of an external field H_z, be $\langle \mu_z \rangle$. The effective interchain exchange field can then be written as $\lambda' \langle \mu_z \rangle$, where

$$\lambda' = 2z' J' / g_z^2 \mu_B^2 \tag{3.2}$$

in which J' is an interchain Heisenberg exchange, z' are the number of interchain nearest-neighbor spins, and $g_z = \langle 2S_z + kL_z \rangle / \langle S_z \rangle$. The isolated-chain susceptibility in the z direction is then given by

$$\chi^z_{\text{chain}} = N \langle \mu_z \rangle / (H_z + \lambda' \langle \mu_z \rangle), \tag{3.3}$$

and is therefore related to the interacting-chain susceptibility $\chi^z = N \langle \mu_z \rangle / H_z$ by

$$(\chi^z)^{-1} = (\chi^z_{\text{chain}})^{-1} - \lambda'/N, \tag{3.4}$$

where there are N spins per mole. For $RbFeCl_3$ there will evidently be two such relationships, one for parallel susceptibility and one for perpendicular susceptibility. For $\Delta'/|\lambda| = 1.1 \pm 0.2$ the corresponding g values are only weakly temperature dependent to low temperatures with values $g_z = g_\parallel \approx 2.6$, $g_\perp \approx 2.8$. Care should be taken to distinguish these "real-spin" g factors from the fictitious spin-1 g factors referred to and used elsewhere in these papers. Using (3.4) with CEF values for the isolated-chain susceptibility allows a best fit to the experimental data for $\Delta'/|\lambda| = 1.3$, $J/|\lambda| = 0.015$, $2z'J'/|\lambda| = -0.038$ and is shown in Fig. 6.

Although the fit seems quite convincing there are reasons for skepticism concerning it. They are as follows: (a) The largest percentage deviations ($\sim$10–15%) occur at the higher-temperature end where the theory should be best, (b) the implied ratio $|J'/J| \approx 0.2$ ($z' = 6$) is a factor of 10 larger than that found using $J/|\lambda| = 0.015$ and interpreting the Curie temperature with the aid of the Oguchi relationship (6.2) of Paper I, and (c) even self-consistently within the theory a long-range antiferromagnetic order would set in when $(\chi^\perp_{\text{chain}})^{-1} = -\lambda'/2N \approx 1.0$ (which is when $T \approx 11\,^\circ$K), at which point the staggered susceptibility diverges for the close-packed hexagonal interchain geometry. In other words the low Néel temperature of about $2.5\,^\circ$K suggests a value of J' much smaller than the value $\approx -0.4\,^\circ$K determined from the fit in Fig. 6. Additional evidence in favor of a smaller J' comes from the crystallography (see Sec. IV), which leads to the expectation that interchain exchange in the chloride should be, if anything, smaller than in the bromide, and from a semi-quantitative analysis of perpendicular susceptibility in the ordered phase. The latter, for a system of weakly interacting chains, is independent of intrachain exchange and, in the fictitious spin-1 language of Paper I, Sec. VI, is given by the expression

$$\chi^\perp(T=0) = g_\perp^2 \mu_B^2 N / 18 J'_\perp, \tag{3.5}$$

in molecular-field approximation (for the triangular spin pattern of ordered $RbFeCl_3$) where $g_\perp \approx 3.7$ and

$J_\perp' = Q^2 J' \approx 2.5 J'$ (see Paper I). Fluctuation effects in lowest order can be included as a well-known modification to the denominator of (3.5) to give[7]

$$\chi^\perp(T=0) = g_\perp^2 \mu_B^2 N/[18 J_\perp'(1+f)], \tag{3.6}$$

where f is the ratio of nearest-neighbor *inter*-chain transverse magnetic moment fluctuation to the square of the spontaneous single-site moment. Although intrachain fluctuation effects are in all probability very large the interchain fluctuations measured by f are likely to be more modest but certainly not negligible. For $f=0$ we use (3.5) with the measured value $\chi^\perp(T=0) = 0.47 \pm 0.02$ emu/mole to deduce an upper limit $J_\perp' \approx -0.5\,^\circ\mathrm{K}$, which is equivalent to $J' \approx -0.2\,^\circ\mathrm{K}$. An Oguchi calculation using $T_N = 2.5\,^\circ\mathrm{K}$, $J \sim 0.01\,|\lambda|$ suggests $J' \approx -0.05\,^\circ\mathrm{K}$.

It therefore seems probable that the fit of theory with experiment shown in Fig. 6 is spurious and that in reality we should not expect a quantitative fit at low temperatures from an approximate theory of the present form. First, from Fig. 4 of Paper I, we should expect the CEF approximation to overestimate susceptibility at lower temperatures. In addition we should not expect a molecular-field inclusion of interchain exchange to be quantitative. In fact, molecular-field theory would be expected to underestimate the J' reduction of paramagnetic susceptibility in the present context. On the other hand we see from Fig. 4 of Paper I that the CEF theory should be accurate to within a percent or two above $y = 3kT/4JS(S+1) \sim 3$. In $RbFeCl_3$ this corresponds to $T \gtrsim 40\,^\circ\mathrm{K}$. An interchain exchange $|J'| \sim 0.1\,^\circ\mathrm{K}$ has a negligible effect on susceptibility at these temperatures and we ought therefore to be able to draw some conclusions from Fig. 5 by fitting theory and experiment at the higher-temperature end (i.e., 50–70 °K). This is achieved when $\Delta'/|\lambda| \approx 1.0$, $J/|\lambda| \approx +0.010$. The discrepancies which develop at lower temperatures are then attributed in varying degrees to (a) the expected over-response of CEF chain theory for low-spin quantum number, (b) the presence of interchain exchange forces, (c) demagnetization corrections, and (d) the possible presence of non-Heisenberg contributions to exchange. The first three of these would be expected to affect the perpendicular susceptibility more seriously than the parallel susceptibility and each would decrease the low-temperature difference between simple theory and experiment. We shall demonstrate below that the presence of the physically most likely non-Heisenberg term would depress the low-temperature parallel susceptibility and again reduce the deviation between theory and experiment. Although our evidence for its importance is perhaps not conclusive, a derivation of the form of this non-Heisenberg term is of interest and will be given in Sec. IV.

For the moment we feel that tentative conclusions within the Heisenberg model can be stated as

$$\Delta'/|\lambda| = 1.1 \pm 0.1, \quad J/|\lambda| = 0.011 \pm 0.004,$$
$$|\lambda| = 130 \pm 10\,^\circ\mathrm{K}, \quad J' = -0.1\,^\circ\mathrm{K}\ (\pm 100\%), \tag{3.7}$$

and contrast very markedly with the estimates of Montano *et al.*[4] (which in our language are $\Delta'/|\lambda| \approx 2.3$, $J/|\lambda| \approx 0.04$) obtained by use of the isolated-pair model. We note in particular that the exchange J in the chloride is ferromagnetic and rather smaller than that of the bromide. This smaller value of exchange $J \sim 1.5\,^\circ\mathrm{K}$ is closer to, but still comfortably larger than, the (molecular-field) critical exchange $J_c \approx 0.6\,^\circ\mathrm{K}$, which is just capable of producing long-range order in this singlet-ground-state situation at absolute zero. The singlet-ground-state effects are therefore expected to be more significant in the chloride but perhaps still not large. The low-temperature spontaneous magnetic moment per Fe^{2+} is,[3] at $\sim 2\mu_B$, a little smaller than in $RbFeBr_3$, but most impressive is the enormous reduction from its formal saturation value $g_\perp \mu_B = 3.7\mu_B$. This reduction is partly a singlet-ground-state effect (i.e., even in molecular-field theory the ground-state moment is reduced from its formal value and, in fact, goes to zero as $J \to J_c$) but in the quasi-linear-chain situation zero-point quantum fluctuations must also be very important. They can be reduced by applying a large magnetic field $\perp c$ to rotate the sublattice magnetizations towards a ferromagnetic alignment. We have achieved magnetizations approaching 95% of theoretical saturation (i.e., $3.5\mu_B$ per magnetic ion) in a field of 60 kOe.[8]

Having obtained crystal-field and exchange-parameter information for $RbFeBr_3$ and $RbFeCl_3$ we shall now examine the crystal structures and attempt to understand the differences at the microscopic level in a physical way. Of particular significance is the ferromagnetic sign of J in the chloride and antiferromagnetic sign in the bromide and possible reasons for a greater importance of non-Heisenberg exchange in the chloride.

IV. EXCHANGE AND CRYSTAL STRUCTURE

The bridging anion structure[9,10] between nearest-neighbor pairs of intrachain and interchain Fe^{2+} ions in $RbFeCl_3$ and $RbFeBr_3$ is shown in Fig. 7. Interchain exchange occurs via a two-anion Fe-X-X-Fe bridge and involves a covalent bonding of magnetic $d\gamma$ (e orbital) electrons with anion p orbitals. Since both d orbitals on each cation are singly occupied in Fe^{2+}, and the orbital degeneracy of e^2 is 1, the resulting exchange is expected to be of simple Heisenberg form between real spins. The greater covalency of the bromine anion over the chlorine anion, coupled with the larger radial extension of bromine and approximately the same X-

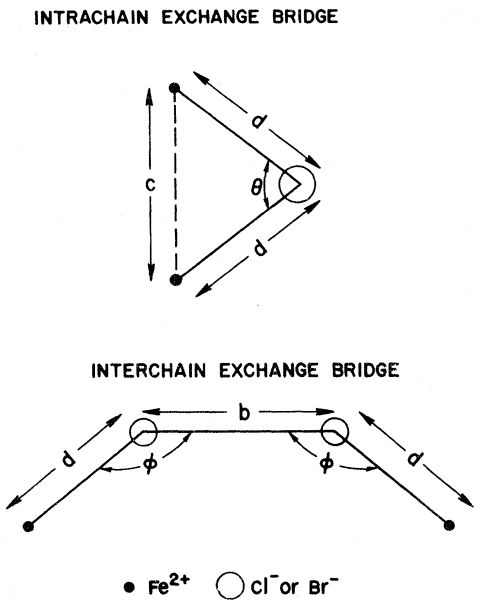

	b	c	d	θ	φ
$RbFeCl_3$[9]	3.67 Å	3.01 Å	2.47 Å	74.7°	133.3°
$RbFeBr_3$[10]	3.74 Å	3.14 Å	2.62 Å	73.3°	134.0°

FIG. 7. Local crystal structure of $RbFeX_3$ (X = Cl, Br) showing the intrachain and interchain ligand bridge structures and some more important values of angular and distance parameters. The bromide parameters refer to the higher-temperature phase. In the low-temperature puckered phase (see Paper I) the two inequivalent sets of parameters straddle the higher-symmetry values given here.

X distance in the two crystals (Fig. 7), would seem to favor a larger interchain exchange J' for $RbFeBr_3$. The slightly larger Fe-X-X angle in the bromide (134° as against 133° in the chloride) would also seem to favor a larger effect in $RbFeBr_3$ since one expects kinetic superexchange to be maximized (and antiferromagnetic) for 180° overlap.

This same e-orbital–to–anion-p-orbital bonding also contributes a Heisenberg superexchange term to nearest-neighbor intrachain exchange via a single Fe-X-Fe bridge. There are three such paths for each cation pair and the Fe-X-Fe bridging angle is 75° in the chloride and 73° in the bromide. These angles are very close to that for which the (ferromagnetic) potential exchange and (antiferromagnetic) kinetic exchange contibutions to superexchange become equal. Potential exchange is always present when there is finite overlap but kinetic exchange, which normally dominates, becomes small for near-orthogonal overlap. Bridge angles greater than 20° removed from a right angle nearly always give rise to an antiferromagnetic resultant and those less than 10° removed from a right angle are nearly always ferromagnetic. The ferromagnetic sign of intrachain exchange in $RbFeCl_3$ and antiferromagnetic sign in $RbFeBr_3$ would seem to conform with this picture although the cancellation angle is not completely independent of the nature of the constituent ions and it is difficult to predict in advance the sign or relative magnitudes of exchange in systems with a 70° – 80° superexchange bridging angle.

As mentioned in Paper I there is a second possibly important exchange path for nearest-neighbor intrachain cations via the direct overlap of c-axis $d\epsilon$ (t_2 orbital) electrons. The relevant Fe-Fe distance is 3.01 Å in the chloride and 3.14 Å in the bromide. This exchange is of kinetic origin and necessarily antiferromagnetic. From the distances involved one would expect it to be larger in the chloride. Most importantly, however, this exchange occurs only when the relevant orbitals are singly occupied in both neighbor Fe^{2+} ions. Let us label the three $d\epsilon$ orbtials according to their $M_{L'}$ quantum number (e.g., $|M_{L'}\rangle$). As far as orbital angular momentum is concerned Fe^{2+} can be treated as having a single electron (in addition to the $3d^5$ closed shell) so that we can indeed use $M_{L'}$ to label single-electron orbitals. Of the three orbitals $|0\rangle$, $|+1\rangle$, $|-1\rangle$, the first has an orbital lobe along the c (or z) axis while $|\pm1\rangle$ are concentrated in the plane normal to the c axis. When the sixth electron is in the $|0\rangle$ orbital this orbital is doubly occupied and no exchange results. On the other hand if both neighbor cations have sixth electrons in $|\pm1\rangle$ orbitals the c-axis lobes are singly occupied and an antiferromagnetic exchange results. We assume therefore that the dominant term in the direct exchange Hamiltonian can be expressed as

$$\mathcal{H}_D = -2J_D L'^2_{iz} L'^2_{jz} \vec{S}_i \cdot \vec{S}_j , \tag{4.1}$$

between cations at sites i and j. Labeling the super-exchange contributions by a parameter J_S the total intrachain exchange Hamiltonian becomes

$$\mathcal{H}_{ex} = \sum_{i>j}\sum - 2(J_S + J_D L'^2_{iz} L'^2_{jz}) \vec{S}_i \cdot \vec{S}_j , \tag{4.2}$$

where J_D is necessarily negative.

Because of its complicated orbitally degenerate form we have not developed the full 15-level ($L' = 1$, $S = 2$) CEF theory for use with (4.2). For simplicity we concentrate on the fictitious spin-1 Hamiltonian pertinent for use when only the lowest three Fe^{2+} eigenlevels are thermally populated. The form of these lowest three states using a basis $|M_{L'}, M_S\rangle$ has been given in Eqs. (4.3) and (4.4) of Paper I. Within these states the matrix elements of $L'^2_z \vec{S}$ and $\vec{S}$ are directly related to those of the fictitious spin $\vec{S}'$ by

$$L'^2_z S_z = R_L S'_z , \quad L'^2_z S^{\pm} = Q_L S'^{\pm} , \tag{4.3}$$

$$S_z = R S'_z , \quad S^{\pm} = Q S'^{\pm} , \tag{4.4}$$

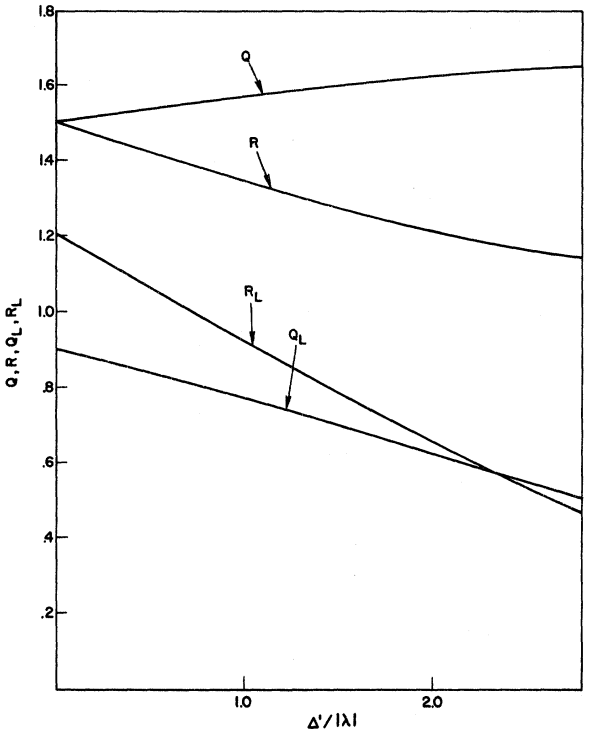

FIG. 8. Parameters Q, R, Q_L, and R_L of Eqs. (4.5) and (4.6), which are required to transform the exchange Hamiltonian to a spin $S'=1$ representation, are shown as a function of trigonal distortion $\Delta'/|\lambda|$.

in which

$$R_L = 2c^2, \qquad Q_L = a'(\sqrt{3}\,a + \sqrt{2}\,c), \tag{4.5}$$

$$R = b^2 + 2c^2, \quad Q = (\sqrt{3}\,aa' + \sqrt{3}\,bb' + \sqrt{2}\,ca'), \tag{4.6}$$

and are plotted numerically as functions of $\Delta'/|\lambda|$ in Fig. 8. Using (4.3) and (4.4) the exchange Hamiltonian (4.2) transforms to

$$\mathcal{H}_{ex} = \sum_{i>j}\sum - 2J_\perp(S'_{ix}S'_{jx} + S'_{iy}S'_{jy}) - 2J_\parallel S'_{iz}S'_{jz}, \tag{4.7}$$

in which

$$J_\perp = Q^2 J_S + Q_L^2 J_D, \quad J_\parallel = R^2 J_S + R_L^2 J_D. \tag{4.8}$$

Writing the splitting between the ground singlet and the first excited doublet as $DS_z'^2$ the final effective-spin-1 Hamiltonian becomes

$$\mathcal{H} = \sum_i [DS_{iz}'^2 - \mu_B \vec{H}\cdot\overleftrightarrow{g}\cdot\vec{S}_i'] + \mathcal{H}_{ex}, \tag{4.9}$$

where H is an applied field, and $\overleftrightarrow{g}$ is diagonal with components $g_\parallel$ and $g_\perp$ parallel and perpendicular to the c axis. D, $g_\parallel$, and $g_\perp$ are *not* free parameters but are all related directly to trigonal distortion $\Delta'/|\lambda|$ as shown in Fig. 9, where an orbital reduction $k=0.87$ has been used for the g calculations.

V. CORRELATED-EFFECTIVE-FIELD APPROXIMATION

Hamiltonian (4.9) is easily approximated in CEF theory. The effective CEF Hamiltonian for the ith spin becomes

$$\mathcal{H}_{i\ \mathrm{eff}} = DS_{iz}'^2 - \mu_B \vec{H}\cdot\overleftrightarrow{g}\cdot\vec{S}_i + 2S_{iz}'^2(J_\perp\alpha_\perp - J_\parallel\alpha_\parallel), \tag{5.1}$$

where the parallel and perpendicular correlation parameters are determined self consistently by solution of

$$\alpha_\parallel = \frac{\int_{-\pi}^{\pi}\cos\theta\,(t_\parallel + \alpha_\parallel - \cos\theta)^{-1}\,d\theta}{\int_{-\pi}^{\pi}(t_\parallel + \alpha_\parallel - \cos\theta)^{-1}\,d\theta}, \tag{5.2}$$

$$\alpha_\perp = \frac{\int_{-\pi}^{\pi}\cos\theta\,(t_\perp + \alpha_\perp - \cos\theta)^{-1}\,d\theta}{\int_{-\pi}^{\pi}(t_\perp + \alpha_\perp - \cos\theta)^{-1}\,d\theta}, \tag{5.3}$$

in which

$$t_\parallel = kT/[4J_\parallel\langle S_\parallel : S_\parallel\rangle]$$

and

$$t_\perp = kT/[4J_\perp\langle S_\perp : S_\perp\rangle],$$

and

$$\langle S_\parallel : S_\parallel\rangle = 2e^{-E/kT}/(1+2e^{-E/kT}), \tag{5.4}$$

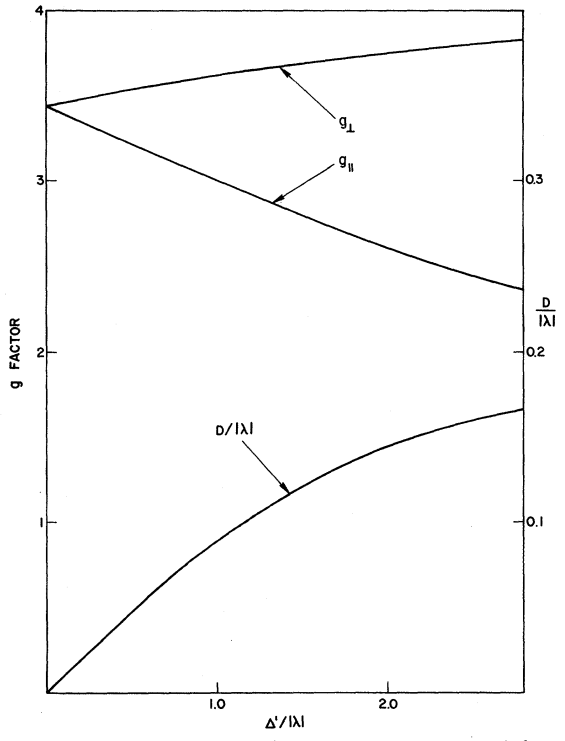

FIG. 9. Crystal-field splitting parameter D and the parallel and perpendicular g factors, which are required for a description of the lowest three crystal-field levels of Fe^{2+} in terms of the fictitious $S'=1$ notation of Eq. (4.9), are shown as functions of trigonal distortion $\Delta'/|\lambda|$.

$$\langle S_\perp : S_\perp \rangle = (2kT/E)(1 - e^{-E/kT})/(1 + 2e^{-E/kT}), \tag{5.5}$$

where E is the singlet-doublet splitting in the correlated approximation, namely,

$$E = D + 2J_\perp \alpha_\perp - 2J_\parallel \alpha_\parallel . \tag{5.6}$$

Equations (5.2) and (5.3) can be integrated analytically to give

$$\alpha_k = -t_k \pm (1 + t_k^2)^{1/2}, \quad k = \parallel, \perp \tag{5.7}$$

the positive sign relevant for positive correlations (J_k positive) and the minus sign for negative correlations (J_k negative). Solving this closed set of equations numerically for $\alpha_\parallel$ and $\alpha_\perp$ the magnetic susceptibility follows as

$$\chi_k = N g_k^2 \mu_B^2 \langle S_k : S_k \rangle / [kT - 4J_k(1 - \alpha_k)\langle S_k : S_k \rangle]. \tag{5.8}$$

One very important omission from (5.8), however, is the temperature-independent Van Vleck contribution to susceptibility. This arises from the matrix elements of angular momentum connecting the three $S' = 1$ eigenstates to the higher levels. For values of $\Delta'/|\lambda| \sim 1.0$ it is close to isotropic and of magnitude 0.011 emu/mole (as calculated by direct comparison of the full and fictitious spin-1 CEF theories with isotropic exchange) and can be added directly to (5.8). Its presence prevents the parallel susceptibility from going to zero at very low temperatures (as seen in Fig. 5) and its neglect has very serious theoretical consequences since it makes up fully 25% of the parallel susceptibility at 70 °K. The neglect of this term by Montano *et al.*[4] causes a very serious overestimate of the relevant g factor, which is an adjustable parameter in that theory.

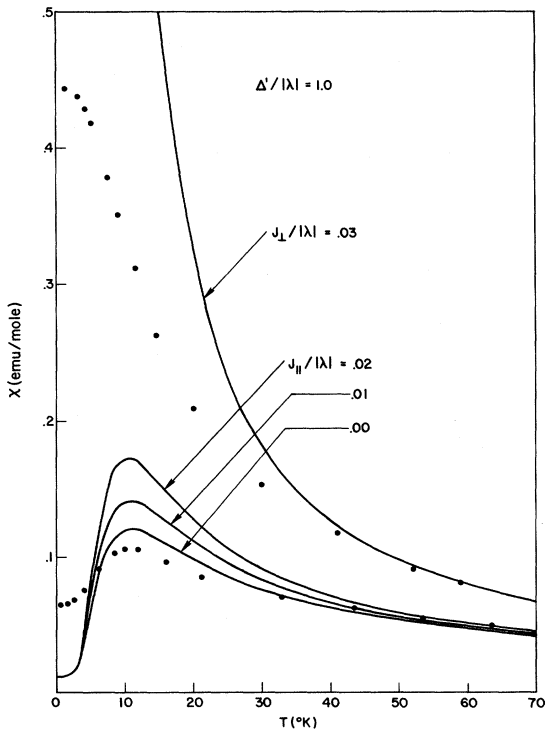

FIG. 10. CEF susceptibility curves for orbitally degenerate exchange, as computed from Eq. (5.8) with $\Delta'/|\lambda| = 1.0$, $|\lambda| = 130$ °K, $g_\parallel = 3.00$, $g_\perp = 3.62$ (and including the Van Vleck term mentioned in the text), are compared with experiment for $RbFeCl_3$. No interchain exchange is included.

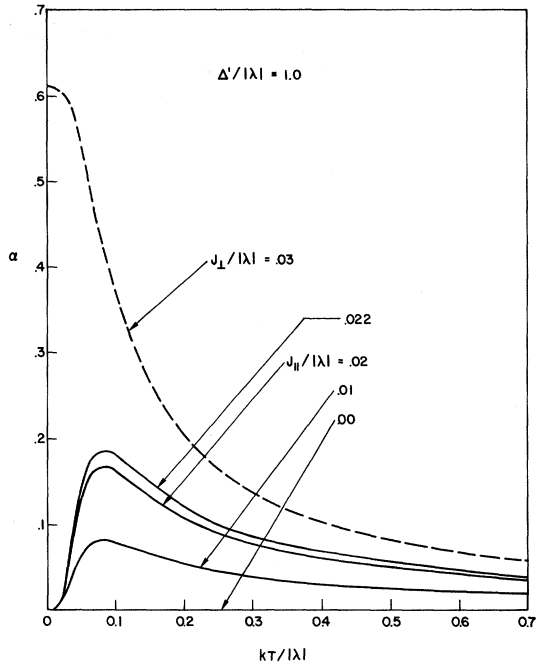

FIG. 11. CEF correlation parameters $\alpha_\perp$ (dashed curve) and $\alpha_\parallel$ (full curves) corresponding to the susceptibility curves of Fig. 10 are plotted as functions of temperature. The perpendicular correlation curve is independent of the $J_\parallel/|\lambda|$ parameter on this scale. Also shown here is the parallel correlation for $J_\parallel/|\lambda| = 0.22$ which is, with $J_\perp/|\lambda| = 0.03$, the value corresponding to isotropic Heisenberg exchange between real spins when $\Delta'/|\lambda| = 1.0$.

Computed curves of $\chi_\parallel$ and $\chi_\perp$ from (5.8) are shown in Fig. 10 for $\Delta'/|\lambda| = 1.0$ ($g_\parallel = 3.00$, $g_\perp = 3.62$), $J_\perp/|\lambda| = 0.03$, and $J_\parallel/|\lambda| = 0.02, 0.01$, and 0. For isotropic exchange J between real spins the equivalent value of $J_\parallel$ when $J_\perp = 0.03|\lambda|$ is $0.022|\lambda|$ [using Fig. 8 and the relationship $J_\perp/J_\parallel = (Q/R)^2$]. The corresponding value of isotropic (real spin) J is $J = 0.012|\lambda| = 1.6$ °K. For fixed $J_\perp$ the perpendicular susceptibility curves are essentially independent of $J_\parallel$ on the scale of Fig. 10. We note that a reduction of $J_\parallel$ from its "isotropic" value rapidly brings the theoretical curves of parallel susceptibility closer to experiment. The temperature-dependent correlation

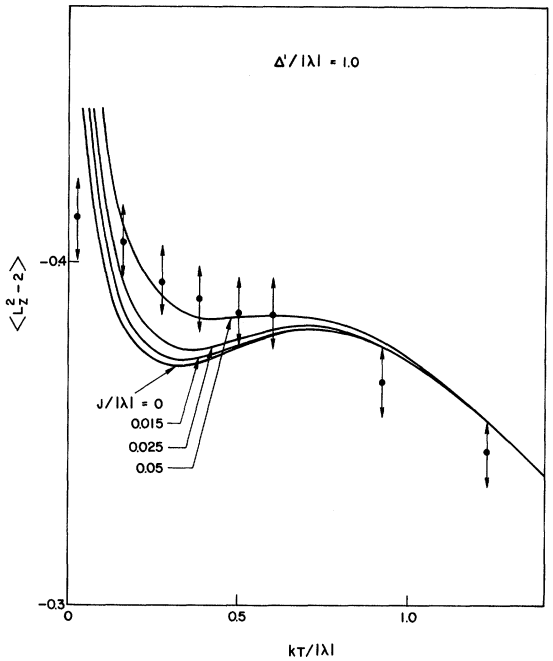

FIG. 12. CEF curves for $\langle L_z^2 - 2 \rangle$, as computed for Heisenberg exchange J and with $|\lambda| = 130\,^\circ\mathrm{K}$, $\Delta'/|\lambda| = 1.0$, are compared with the low-temperature experimental quadrupole splitting data (filled circles plus error bars) thereby extending the comparison in Fig. 3 to lower temperatures for which exchange effects become significant.

parameters $\alpha_\parallel$ and $\alpha_\perp$ for the non-Heisenberg situation are shown in Fig. 11.

VI. CONCLUSIONS

Using the simplest model Hamiltonian (3.1), with isotropic intrachain exchange between real spins, a quantitative fit to experiment for both quadrupole splitting and single-crystal susceptibility has been obtained in $RbFeCl_3$ only at temperatures above about 60 °K. Below this temperature discrepancies develop. Some of them have an obvious physical explanation. For example, the theoretical $\chi_\perp$ tends to large values as $T \to 0$, reflecting an incipient ferromagnetic alignment due to the ferromagnetic J. Experimentally the divergence is prevented by the weak interchain J'. An effective-field theory is too crude to assess the J' effects quantitatively but the qualitative trend is apparent and as a crude estimate $J' \sim -0.1\,^\circ\mathrm{K}$ is obtained.

The discrepancy between experiment and theory for $\chi_\parallel$ has a different origin. Effects of J' and probable inaccuracy of CEF theory can only account for a small part of the low-temperature $\chi_\parallel$ discrepancy and we suggest that the remaining part is evidence for the existence of a non-Heisenberg exchange (Sec. IV). In the fictitious spin notation exchange values $J_\perp \approx 0.03|\lambda|$ and $J_\parallel \approx 0.005|\lambda|$ would account for the remaining discrepancy in a qualitative fashion (Fig. 10).

At room temperature these non-Heisenberg terms will reduce $\chi_\parallel$ from its Heisenberg value leading to an increase in $\chi_\parallel^{-1} - \chi_\perp^{-1}$ and making the estimate $\Delta'/|\lambda| \approx 1.1$ from Fig. 4 an upper bound. A lower bound can be obtained from Fig. 3 where quadrupole splitting ΔE_Q is fitted to the expression $A\langle L_z^2 - 2 \rangle + B$. Theoretically

$$A = \tfrac{1}{7} e^2 Q \langle R^{-3} \rangle , \tag{6.1}$$

where e is electronic charge, $Q \approx 0.21 \times 10^{-24}$ cm^2 is the nuclear quadrupole moment, and $\langle R^{-3} \rangle$ is a shielded radial distribution of magnetic electrons. The free-ion value $\langle R^{-3} \rangle \approx 5.1$ a.u. can be taken as a maximum possible value and leads to the inequality

$$E_Q < [3.05 \langle L_z^2 - 2 \rangle + B] \ \text{mm/sec}. \tag{6.2}$$

From Fig. 3 of this paper and Fig. 8 of Paper I we conclude that $\Delta'/|\lambda| > 0.9$ so that our assumed value $\Delta'/|\lambda| = 1.0$ in Fig. 10 is indeed realistic.

We conclude that direct exchange is possibly important in $RbFeCl_3$. Using $J_\perp \approx 0.03|\lambda|$ and $J_\parallel \approx 0.005|\lambda|$ in (4.8) for $\Delta'/|\lambda| = 1.0$ we find values $J_S \approx 3\,^\circ\mathrm{K}$ and $J_D \approx -5\,^\circ\mathrm{K}$ for ligand superexchange and direct c-axis exchange, respectively. Additional support for the importance of J_D can also be found from analyzing the low-temperature quadrupole splitting. The isotropic Heisenberg estimates of $\langle L_z^2 - 2 \rangle$ for $\Delta'/|\lambda| = 1.0$ and various values of exchange J are shown in Fig. 12. Fit to experiment requires $J/|\lambda| \geq 0.05$ compared to the susceptibility estimate $J/|\lambda| \approx 0.011$. In the non-Heisenberg formalism an antiferromagnetic J_D increases correlation anisotropy $\alpha_\perp - \alpha_\parallel$ dramatically (Fig. 11) and, since the exchange shift of $\langle L_z^2 - 2 \rangle$ is closely proportional to $(\alpha_\perp - \alpha_\parallel) J$ in the Heisenberg picture, this suggests that the above discrepancy would be reduced rapidly by the introduction of J_D. Although quantitative estimates require a development of the non-Heisenberg formalism in the upper energy levels we conclude that the lower-temperature ΔE_Q measurements are not consistent with a Heisenberg formalism and can be construed as supportive evidence for the importance of orbitally degenerate exchange.

ACKNOWLEDGMENTS

We are grateful to D. E. Cox for providing the $RbFeCl_3$ crystals used in this study and to E. Cohen, D. E. Cox, G. R. Davidson, M. D. Sturge, L. R. Walker, and G. K. Wertheim for helpful discussions.

[1]D. E. Cox and F. C. Merkert, J. Cryst. Growth 13/14, 282 (1972).
[2]P. Zory, Phys. Rev. 140, A1401 (1965).
[3]G. R. Davidson, M. Eibschütz, D. E. Cox, and V. J. Minkiewicz, AIP Conf. Proc. 5, 436 (1971).
[4]P. A. Montano, E. Cohen, H. Shechter, and J. Makovsky, Phys. Rev. B 7, 1180 (1973).
[5]M. E. Lines, Phys. Rev. B 9, 3927 (1974).
[6]N. Achiwa, J. Phys. Soc. Jpn. 27, 561 (1969).
[7]M. E. Lines, Phys. Rev. 135, A1335 (1964).
[8]G. W. Hull, Jr. (private communication).
[9]H. J. Seifert and K. Klatyk, Z. Anorg. Allg. Chem. 342, 1 (1966).
[10]M. Eibschütz, G. R. Davidson, and D. E. Cox, AIP Conf. Proc. 18, 386 (1973).